Inorg. Chem. **2007**, *46*, 5343–5348

Solution–Chemical Synthesis of Carbon Nanotube/ZnS Nanoparticle Core/Shell Heterostructures

Feng Gu,* Chunzhong Li,* and Shufen Wang

Key Laboratory for Ultrafine Materials of Ministry of Education, School of Materials Science and Engineering, East China University of Science & Technology, Shanghai 200237, PR China

Received March 13, 2007

A facile solution–chemical method has been developed to be capable of encapsulating a multiwalled carbon nanotube (MWCNT) with ZnS nanocrystals without using any bridging species. The thickness of the ZnS shell can be tuned easily by controlling the experimental conditions. The optical properties of the MWCNT/ZnS heterostructures were investigated using UV–vis absorption and photoluminescence spectroscopy. The optical absorption spectrum indicates that the band gap of ZnS nanocrystallites is 4.2 eV. On the basis of the photoluminescence spectrum, charge transfer is thought to proceed from ZnS nanocrystals to the nanotube in the ZnS–carbon nanotube system. These special heterostructures are very easily encapsulated within a uniform silica layer by a modified-Stöber process and still show better stability even after heat treatment at 400 °C, which makes them appealing for practical applications in biochemistry and biodiagnostics.

Introduction

The discovery of the carbon nanotube has opened a challenging new field in materials, solid-state physics, and chemistry, offering a wide perspective for many possible applications.[1,2] Nowadays, a great deal of research efforts have been devoted to explore novel strategies that can alter the physical properties of carbon nanotubes (CNTs) by surface modification with organic, inorganic and biological species.[3−11] These functional CNT-based composites show eminent prospects and opportunities for new applications in a wide variety of areas. Among them, linking semiconductor nanocrystals to CNTs has emerged as an active field.[7−16] The superiority of this system lies in the fact that the combination of the properties of two functional nanoscale materials can be used to achieve a wider range of applications.[17−23] Also, the electronic interaction between CNTs and the external active semiconductor layer is believed to be of equal importance because it plays a crucial role in constructing optoelectronic devices.[16,24] Several strategies have been

* To whom correspondence should be addressed. E-mail address: czli@ecust.edu.cn (C.L.); gufeng@ecust.edu.cn (F.G.). Fax: +86 21 64250624.

(1) Iijima, S. *Nature* **1991**, *354*, 56.
(2) Rueckes, T.; Kim, K.; Joselevich, E.; Tseng, G. Y.; Cheung, C. L.; Lieber, C. M. *Science* **2000**, *289* (5476), 94.
(3) Li, Q. W.; Sun, B. Q.; Kinloch, I. A.; Zhi, D.; Sirringhaus, H.; Windle, A. H. *Chem. Mater.* **2006**, *18* (1), 164.
(4) Shi, D.; Lian, J.; Wang, W.; Liu, G.; He, P.; Dong, Z.; Wang, L.; Ewing, R. C. *Adv. Mater.* **2006**, *18* (2), 189.
(5) Chen, R. J.; Zhan, Y. G.; Wang, D. W.; Dai, H. J. *J. Am. Chem. Soc.* **2001**, *123* (16), 3838.
(6) Azamian, B. R.; Davis, J. J.; Coleman, K. S.; Bagshaw, C. B.; Green, M. L. H. *J. Am. Chem. Soc.* **2002**, *124* (43), 12664.
(7) Fu, L.; Liu, Z. M.; Liu, Y. Q.; Han, B. X.; Hu, P. G.; Cao, L. C.; Zhu, D. B. *Adv. Mater.* **2005**, *17* (2), 217.
(8) Du, J. M.; Fu, L.; Liu, Z. M.; Han, B. X.; Li, Z. H.; Liu, Y. Q.; Sun, Z. Y.; Zhu, D. B. *J. Phys. Chem. B* **2005**, *109* (26), 12772.
(9) Joo, J.; Na, H. B.; Yu, T.; Yu, J. H.; Kim, Y. W.; Wu, F. X.; Zhang, J. Z.; Hyeon, T. *J. Am. Chem. Soc.* **2003**, *125* (36), 11100.
(10) Banerjee, S.; Wong, S. S. *Nano Lett.* **2002**, *2* (3), 195.
(11) Zhao, L. P.; Gao, L. *J. Mater. Chem.* **2004**, *14* (6), 1001.
(12) Lee, S. W.; Sigmund, W. M. *Chem. Commun.* **2003**, (6), 780.
(13) Banerjee, S.; Wong, S. S. *J. Am. Chem. Soc.* **2003**, *125* (34), 10342.
(14) Haremza, J. M.; Hahn, M. A.; Krauss, T. D. *Nano Lett.* **2002**, *2* (11), 1253.
(15) Ravindran, S.; Chaudhary, S.; Colburn, B.; Ozkan, M.; Ozkan, C. S. *Nano Lett.* **2003**, *3* (4), 447.
(16) Cao, J.; Sun, J. Z.; Hong, H.; Li, H. Y.; Chen, H. Z.; Wang, M. *Adv. Mater.* **2004**, *16* (1), 84.
(17) Daniel, M. C.; Astruc, D. *Chem. Rev.* **2004**, *104* (1), 293.
(18) Kong, J.; Franklin, N. R.; Zhou, C. W.; Chapline, M. G.; Peng, S.; Cho, K. J.; Dai, H. J. *Science* **2000**, *287* (5453), 622.
(19) Robel, I.; Bunker, B. A.; Kamat, P. V. *Adv. Mater.* **2005**, *17* (20), 2458.
(20) Correa-Duarte, M. A.; Perez-Juste, J.; Sanchez-Iglesias, A.; Giersig, M.; Liz-Marzan, L. M. *Angew. Chem., Int. Ed.* **2005**, *44* (28), 4375.
(21) Correa-Duarte, M. A.; Grzelczak, M.; Salgueirino-Maceira, V.; Giersig, M.; Liz-Marzan, L. M.; Farle, M.; Sierazdki, K.; Diaz, R. *J. Phys. Chem. B* **2005**, *109* (41), 19060.
(22) Tessler, N.; Medvedev, V.; Kazes, M.; Kan, S. H.; Banin, U. *Science* **2002**, *295* (5559), 1506.
(23) Planeix, J. M.; Coustel, N.; Coq, B.; Brotons, V.; Kumbhar, P. S.; Dutartrc, R.; Gcncstc, P.; Ajayan, P. M. *J. Am. Chem. Soc.* **1994**, *116*, 7935.
(24) Strano, M. S.; Dyke, C. A.; Usrey, M. L.; Barone, P. W.; Allen, M. J.; Shan, H. W.; Kittrell, C.; Hauge, R. H.; Tour, J. M.; Smalley, R. E. *Science* **2003**, *301* (5639), 1519.

10.1021/ic7004858 CCC: $37.00
Published on Web 05/25/2007

developed for the synthesis of CNT/semiconductor heterostructures.[12−16] However, most current methods of binding semiconductor nanocrystals to CNTs often make use of small organic bridging molecules to improve the adhesion between the nanocrystals and CNTs.[7,15,16,25−28] This not only complicates the synthesis but also results in indirect and poorer contact between the different phases. The resulting increase in the barrier for electron transport can adversely affect the material's performance in optoelectronic applications.[24]

Of the various types of nanocrystals, semiconducting metal chalcogenide nanocrystals have been the most intensively studied because of their quantum confinement effects and size- and shape-dependent photoemission characteristics. These semiconductor nanocrystals have been applied to many different technological areas, including biological labeling and diagnostics, light emitting diodes, photovoltaic devices, and lasers.[29−33] Many semiconducting nanocrystals of metal sulfides with various compositions and shapes have been synthesized. As an important group II−VI semiconductor with a band gap of 3.6 eV, ZnS has been used widely in displays, sensors, and lasers for many years.[34−36] Functionalizing CNTs with ZnS nanocrystals can not only combine the advantages of ZnS and CNTs but also may result in new properties, which have potential applications in nanoscale electronic devices. Several approaches have been put forward for the synthesis of CNT/ZnS heterostructures.[8,11,15] Such approaches, though successful in the formation of nanoscaled heterostructures, were both complex and difficult to control. Therefore, it is desirable to explore facile routes for the synthesis of CNT/ZnS heterostructures with promising novel properties, especially such methods that may be easily controllable, easily repeatable, mild, and feasible. In this Article, we demonstrate a facile solution−chemical route for large-scale synthesis of uniform ZnS-coated carbon nanotubes without using any bridging species. Accordingly, the elimination of barrier-to-electron transport would facilitate the material's performance in optoelectronic applications. By varying the experimental parameters, the ZnS layer can be adjusted properly. The formation mechanism of these heterostructures has been studied systematically.

The stability of nanoscale materials is a key factor influencing their applications. Nanoscale materials often display high chemical reactivity due to their low dimensionality and a high surface-to-volume ratio. This chemical reactivity leads to deformation, oxidation, and contamination of the nanoscale materials, resulting in dramatic changes in their structures and properties. One solution to the problem is to coat them with inert protective sheaths.[37−40] These CNT/ZnS nanostructures would benefit from having a silica shell to overcome the oxidation difficulty. Furthermore, silica-coated nanostructures are very useful for biological applications because they allow for surface conjugation with amines, thiols, and carboxyl groups, which in turn would facilitate the linking of biomolecules such as biotin and avidin. On the other hand, incorporation of luminescent nanomaterials into nanotubes has been explored as a way to prepare bright biological labels and functional composite luminescent materials.[21] Herein, silica-coated MWCNT/ZnS heterostructures were prepared. The coating process is very simple without any "surface decoration", involving a modified-Stöber process, which makes them appealing for practical applications in biochemistry and biodiagnostics.

Table 1. Summary of the Experimental Conditions and Results of the Resultant MWCNT/ZnS Samples[a]

sample	A	B	C	D	E	F	G
TAA (g)	4.00	4.00	4.00	5.00	5.00	5.00	4.00
time (h)	2	4	6.5	2	4	6.5	4
shell thickness (nm)	12	15	20	18	23	25	13

[a] In the above-mentioned experiments, 1.10 g $Zn(Ac)_2$ and 0.10 g MWCNT were used. Sample G was prepared without sonication process and the other experimental conditions were analogous.

Experimental Section

Multiwalled carbon nanotubes (MWCNTs) were provided by the Shenzhen Nanoport Company and were used without any acid treatment. In a typical experiment, to prepare the MWCNT/ZnS heterostructures, 0.10 g of MWCNTs (diameter of 40−60 nm) was dispersed in 100 mL of distilled water with the aid of ultrasonication (100 W, 40 kHz) for 10 min. Subsequently, 1.10 g of zinc acetate ($Zn(CH_3COO)_2 \cdot 2H_2O$, A.R.) and 5.00 g of thioacetamide (TAA, A.R.) were added to the mixture and stirred for 30 min. Then, the mixture was heat-treated at 45 °C for 4 h. The as-obtained samples were filtered and then washed with absolute ethanol and distilled water several times to remove possible residual impurities. The products were dried at 60 °C in a vacuum oven before being further characterized. The detailed experimental parameters and their influence on the thickness of the ZnS shell are listed in Table 1. Coating of the MWCNT/ZnS heterostructures with SiO_2 has been achieved using a versatile modified-Stöber process with the aid of sonication. Typically, 0.10 g of the obtained MWCNT/ZnS sample was added to 50 mL of ethanol and sonicated for 15 min. Then, 5 mL of $NH_3 \cdot H_2O$ (26%) and a certain amount of tetraethyl orthosilicate (TEOS, A.R.) were added subsequently. After being held for 1.5 h under sonication without any cooling, the products were obtained by centrifugation, washed for several times, and then vacuum-dried.

(25) Shi, J. H.; Qin, Y. J.; Wu, W.; Li, X. L.; Guo, Z. X.; Zhu, D. B. *Carbon* **2004**, *42* (2), 455.
(26) Zhu, Y. C.; Bando, Y.; Xue, D. F.; Golberg, D. *J. Am. Chem. Soc.* **2003**, *125* (52), 16196.
(27) Lordi, V.; Yao, N.; Wei, J. *Chem. Mater.* **2001**, *13* (3), 733.
(28) Liu, B.; Lee, J. Y. *J. Phys. Chem. B* **2005**, *109*, 23783.
(29) Huang, J. X.; Xie, Y.; Li, B.; Liu, Y.; Qian, Y. T.; Zhang, S. Y. *Adv. Mater.* **2000**, *12* (11), 808.
(30) Lee, S. M.; Jun, Y. W.; Cho, S. N.; Cheon, J. *J. Am. Chem. Soc.* **2002**, *124* (38), 11244.
(31) Yu, S. H.; Yoshimura, M. *Adv. Mater.* **2002**, *14* (4), 296.
(32) Ma, Y.; Qi, L.; Ma, J.; Cheng, H.; Shen, W. *Langmuir* **2003**, *19*, 9079.
(33) Sone, E. D.; Zubarev, E. R.; Stupp, S. I. *Angew. Chem., Int. Ed.* **2002**, *41* (10), 1705.
(34) Prevenslik, T. V. *J. Lumin.* **2000**, *87*−*89*, 1210
(35) Zhao, Y. W.; Zhang, Y.; Zhu, H.; Hadjipianayis, G. C.; Xiao, J. Q. *J. Am. Chem. Soc.* **2004**, *126* (22), 6874.
(36) Falcony, C.; Garcia, C.; Ortiz, A.; Alonso, J. C. *J. Appl. Phys.* **1992**, *72* (4), 1525.
(37) Shen, G.; Bando, Y.; Golberg, D. *J. Phys. Chem. B* **2006**, *110*, (42), 20777.
(38) Jiang, Y.; Meng, X. M.; Liu, J.; Hong, Z. R.; Lee, C. S.; Lee, S. T. *Adv. Mater.* **2003**, *15* (14), 1195.
(39) Jiang, Y.; Meng, X. M.; Liu, J.; Xie, Z. Y.; Lee, C. S.; Lee, S. T. *Adv. Mater.* **2003**, *15* (4), 323.
(40) Shelimov, K. B.; Moskovits, M. *Chem. Mater.* **2000**, *12* (1), 250.

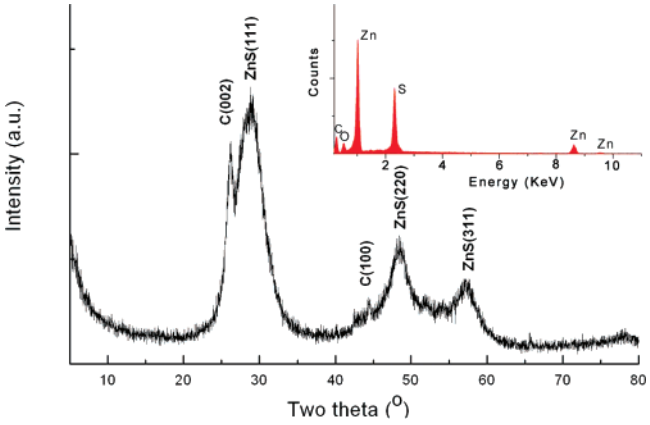

Figure 1. XRD pattern of the formed MWCNT/ZnS heterostructures. Inset shows the EDS spectrum of the sample.

The X-ray diffraction (XRD) patterns of the samples were measured using a Japan Rigaku D/max 2550 VB/PC diffractometer with Cu Kα radiation ($\lambda = 0.15418$ nm). Transmission electron microscope (JEM-100CXII) and a high-resolution transmission electron microscope (JEM-2100) were also used to characterize the products. Scanning electron micrograph (SEM) images were taken with a FEI SIRION-200 scanning electron microscope. The Fourier transform infrared (FTIR) spectra of the samples were collected using a Nicolet Magna-550 infrared spectrometer. Raman scattering spectra were measured with a LabRam 1B micro-Raman spectrometer at room temperature. The 632.8 nm line of a He−Ne laser was used for the excitation. Diffuse reflectance spectra (DRS) were obtained for the dry-pressed disk samples using a Scan UV−vis-NIR spectrophotometer (Varian, Cary 500) equipped with an integrating sphere assembly. The excitation and photoluminescence (PL) spectra of the sample were measured with a Jobin Fluorolog-3-p spectrophotometer with a Xe lamp at room temperature.

Results and Discussion

The phase purity of the products was characterized by X-ray diffraction (XRD) (Figure 1). The diffraction peaks identify the sample as a mixture of the cubic phase of ZnS (space group, $F\bar{4}3m$, JCPDS 05−0566) with a lattice constant of $a = 5.29$ Å and MWCNTs. The reflection at $2\theta = 26.18°$ arising from the MWCNTs corresponds to the 002 crystal plane, similar to the pristine MWCNTs. The peaks at scattering angles of 29.22, 48.54, and 57.22° correspond to the reflections from the 111, 220, and 311 crystal planes, respectively, of cubic ZnS. The broadening of the diffraction peaks reveals the smaller particle size of the ZnS specimens. The average crystallite size roughly estimated on the basis of the Scherrer formula is about 3 nm. The energy-dispersive spectrometry (EDS) results for the sample reveal the presence of C, Zn, and S in the products (inset of Figure 1). A relatively weak oxygen peak in the spectrum probably originates from the unavoidable surface-adsorption of oxygen onto the samples from exposure to air during sample processing. The FTIR spectrum (Figure S1) of the formed MWCNT/ZnS heterostructures was obtained to determine the structure of the chemical groups formed on the nanotube sidewalls. The absorption at 1569 cm^{-1} is associated with the vibration of the carbon skeleton of the carbon nanotubes.[11,41] The absorption at 1633 cm^{-1} is assigned to the bending vibrations of adsorbed molecular water.

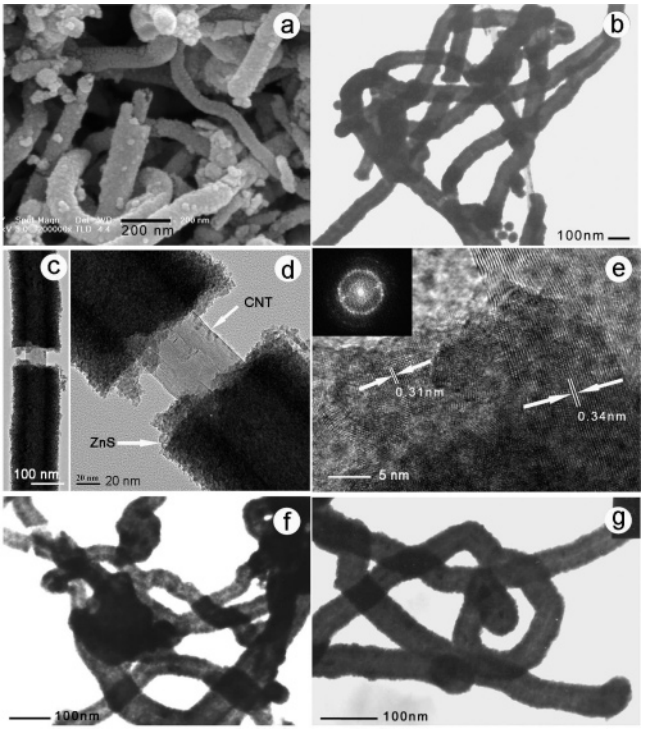

Figure 2. (a,b) SEM and TEM images of the formed MWCNT/ZnS heterostructures (sample C), (c,d) selected high-magnification TEM images of the MWCNT/ZnS heterostructures exhibiting a discrete ZnS layer, (e) HRTEM image of the formed MWCNT/ZnS heterostructures. Inset of e is the corresponding processed FFT, and (f,g) TEM images of samples D and B.

The morphology and microstructure of the samples were examined by scanning electron microscopy (SEM), transmission electron microscopy (TEM), and high-resolution transmission electron microscopy (HRTEM). SEM images reveal that the product appears to be core−shell in structure. The thickness is uniform along the axis of a carbon nanotube. A typical SEM image shown in Figure 2a reveals one composite nanowire with a naked end, showing a coaxial structure of the product. TEM images shown in parts b, f, and g of Figure 2 clearly demonstrate a sharp contrast between the outer and inner layer in the axis direction, which suggests that there is a different phase composition in the radial direction of the wires. For better identification of the formed special core/shell heterostructure, Figure S2 shows the TEM image of the used MWCNTs. It is clear that the MWCNTs are endless with a rather smooth surface. In addition, Figure 2c also shows a selected TEM image of the MWCNT/ZnS heterostructures with a discrete ZnS layer, and the enlarged image is shown in Figure 2d. From these figures, the inner MWCNT as well as the outer formed ZnS layer can be observed apparently. It should be noted that the ZnS layer is constructed of nanoparticles about 3 nm in diameter, which is consistent with the XRD results. The adhesion of the ZnS shell to the MWCNTs was very strong and could not be detached from the latter, even after prolonged sonication.

(41) Liu, L. Q.; Qin, Y. J.; Guo, Z. X.; Zhu, D. B. *Carbon* **2003**, *41* (2), 331.

HRTEM was employed to investigate the inner structure of the MWCNT/ZnS heterostructures, showing that the external layer was composed of small ZnS nanoparticles with an average diameter of 3 nm (Figure 2e). Fast Fourier transform (FFT) analysis of selected regions of the coating can reveal details of the local ZnS structure. The inset to Figure 2e is the corresponding FFT diffraction pattern, which can be indexed to cubic ZnS. The concentric rings could be assigned as diffractions from 111, 220, and 311 planes of face-center-cubic (fcc) ZnS from the centermost ring, respectively. Detailed analysis on the lattice fringes gives an interplanar spacing of 0.31 and 0.34 nm, which match well with the 111 and 002 plane separations of the standard bulk zinc blende ZnS and MWCNTs, respectively.

To understand the formation of MWCNT/ZnS heterostructures better, a series of controlled experiments were carried out. In the absence of MWCNTs, only spherical ZnS nanoparticles can be obtained, as shown in Figure S3. In view of the low-energy point, the MWCNTs are apparently capable of offering optimal nucleation sites. The formation of spherical ZnS particles can be attributed to the oriented aggregation of the initially formed ZnS nanocrystals. The encapsulation condition has also been found to be strongly dependent on the utilization of ultrasonication. Without the aid of ultrasonication, the morphology of the samples varied greatly (Figure S4). The MWCNTs were not well encapsulated by the ZnS, and independent ZnS nanocrystals were also formed in the products. Ultrasonication has been used previously to shorten carbon nanotubes,[42] and a recent study also used it to treat nitrogen-doped carbon nanotubes for ionic adsorption of Au nanoparticles.[43] Ultrasound can produce extremely high local temperatures (~5000 K) due to the implosive collapse of liquid bubbles.[44] They may expedite the surface-modification process of carbon nanotubes. Figure S5 shows the Raman spectra of a MWCNT sample before and after sonication. The intensity of the peak at 1324 cm^{-1}(D band), which is assigned to the amorphous carbon or fine graphitic particles, was greatly reduced after ultrasonication, indicating that the MWCNTs have been "cleaned" greatly. The ultrasonication process modified and activated the surface of the MWCNTs, which would offer suitable nucleation sites for the subsequent growth process. Therefore, the ultrasonication process can be considered as the dominant factor for the synthesis of well-defined MWCNT/ZnS heterostructures. Furthermore, the thickness of the ZnS shell could be readily controlled by changing experimental parameters such as the initial concentration of TAA and reaction time. By suitably adjusting these parameters, the thickness of ZnS shell will change simultaneously. These parameters and their influence on the thickness of the ZnS shell are listed in Table 1. Using smaller amounts of TAA with the other experimental conditions unchanged resulted in the formation of a thinner ZnS shell. For example, when the amount of TAA was decreased from 5.00 to 4.00 g, the thickness of the ZnS shell would change from 23 to 15 nm. When the reaction time was increased from 2 to 6.5 h, the thickness of the ZnS layer changed from 18 to 25 nm.

The MWCNT/ZnS herterostructures were synthesized by a mild solution−chemical reaction using TAA and $Zn(CH_3COO)_2$ as S^{2-} and Zn^{2+} sources, respectively, as well as using MWCNT as a substrate. In comparison with previous studies on metal−sulfide nanoparticles, the probable reaction process for the formation of MWCNT/ZnS heterostructures can be summarized as follows:

$$CH_3CSNH_2 + H_2O \rightarrow CH_3CONH_2 + H_2S$$

$$H_2S \rightarrow H^+ + HS^- \rightarrow 2H^+ + S^{2-}$$

$$Zn^{2+} + S^{2-} \rightarrow ZnS_{(particle)}$$

$$nZnS_{(particle)} + MWCNT \rightarrow MWCNT/ZnS$$

Under the experimental conditions, the positive metal ions Zn^{2+} can be first adsorbed onto the surface of MWCNTs because of electrostatic attraction.[7] The immobilization of Zn^{2+} ions allows heterogeneous nucleation along with the release of S^{2-} from TAA at elevated temperatures, which can be catalytic toward the decomposition of TAA, leading to the formation of primary ZnS particles around the sites. As a result of the relatively lower reaction temperature, primary ZnS nanocrystals can also be formed gradually under a condition of homogeneous nucleation in the aqueous solutions. Through oriented aggregation of the formed primary ZnS nanocrystals, MWCNT/ZnS heterostructures would be formed. The main driving force for oriented aggregation of the nanocrystals was attributed to the tendency to decrease the high surface energy. Through the rotations of the primary ZnS nanocrystals caused by various interactions such as Brownian motion and the short-range interactions between adjacent surfaces, oriented aggregation can be realized.[45−47] It is known that oriented aggregation only requires a 2D structural accord within the plane of the approaching surfaces,[48,49] and the lattice continuity among attached crystals has been confirmed by HRTEM results. Increasing reaction time will lead to the formation of the thicker ZnS shell, and a uniform layer was finally formed over the entire external MWCNT surface at steady state.

Optical studies were carried out to evaluate the crystallization degree and potential optical properties of the as-prepared MWCNT/ZnS composites. The absorption spectrum of MWCNTs is rather featureless in the measured region. Figure S6 shows the UV−vis absorption spectrum of the MWCNT/ZnS composites. After ZnS coating, a dominant absorption peak at 293 nm can be observed, which is considerably blue-shifted from 340 nm for bulk zinc blende

(42) Xing, Y. C. *J. Phys. Chem. B* **2004**, *108* (50), 19255.
(43) Jiang, K.; Eitan, A.; Schadler, L.; Ajayan, P. M.; Siegel, R. W.; Grobert, N.; Mayne, M.; Reyes-Reyes, M.; Terrones, H.; Terrones, M. *Nano Lett.* **2003**, *3* (3), 275.
(44) Suslick, K. S.; Hyeon, T.; Fang, M. *Chem. Mater.* **1996**, *8* (8), 2172.
(45) He, T.; Chen, D. R.; Jiao, X. L. *Chem. Mater.* **2004**, *16* (4), 737.
(46) Banfield, J. F.; Welch, S. A.; Zhang, H. Z.; Ebert, T. T.; Penn, R. L. *Science* **2000**, *289* (5480), 751.
(47) Alivisatos, A. P. *Science* **2000**, *289* (5480), 736.
(48) Gu, F.; Li, C. Z.; Wang, S. F.; Lu, M. K. *Langmuir* **2006**, *22* (3), 1329.
(49) Penn, R. L. *J. Phys. Chem. B* **2004**, *108* (34), 12707.

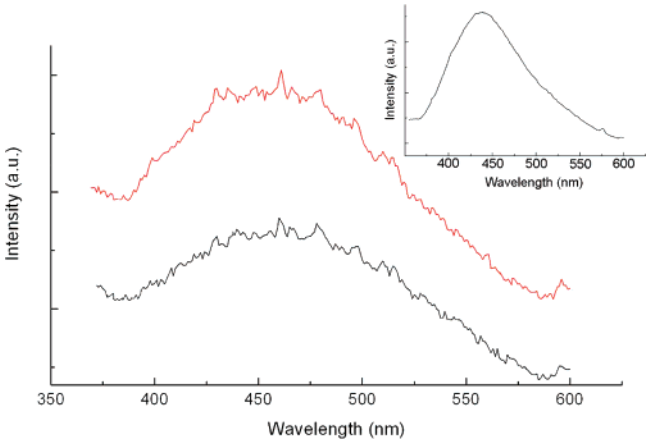

Figure 3. Room-temperature PL spectra of the formed MWCNT/ZnS (black line) and MWCNT/ZnS/SiO_2 (red line) heterostructures. Inset shows the spectrum of the ZnS nanoparticles.

ZnS because of quantum size effects. According to the experimental correlation between the position of the maximum of the absorption and the size of the nanocrystal,[50,51] the particle size of the ZnS nanocrystals is estimated to be 3.2 nm. It has been documented that the optical absorption of ZnS nanocrystals with a size of 4 nm exhibits an excitonic peak at 305 nm,[52] and the presented variation of the band gap versus the size of the ZnS nanocrystallites indicates that an excitonic peak at 293 nm, corresponding to a band gap of 4.2 eV, would correspond to a ZnS nanocrystallite size of about 3 nm, which is consistent with the XRD and HRTEM results. Figure 3 gives the photoluminescence (PL) spectrum of MWCNT/ZnS heterostructures. For comparison, the spectrum of the pristine ZnS nanospheres is also included. It is clear that one dominant emission band centered at 438 nm can be observed, corresponding to the trap-states emission of ZnS nanocrystals as a result of the broad feature and substantial red shift of the band.[8,9] After coating MWCNTs with ZnS, a broad and weak emission band peaking at 454 nm can be obtained with an apparent red shift of about 16 nm. Previous studies indicated that CNTs can act as energy sinks in an excited-state energy transfer mechanism due to the effect of the electron acceptors of CNTs.[8,19] The broadening of the PL spectral response indicates that there is a significant ground-state interaction between ZnS nanocrystals and MWCNTs.[53] Therefore, it can be concluded that electrons from the external ZnS nanocrystals will flow into the inner MWCNTs to form an accumulation layer of electrons, suggesting potential applications for highly efficient photoelectrochemical cells.[8] The direct adhesion between the nanocrystals and CNTs would affect the structure of the adherent ZnS, inevitably with the formation of some local energy levels in the band gap, resulting in the red shift of the emission peak. An investigation into the mechanism of the influence of carbon nanotubes on the optical properties is in progress.

(50) Calandra, P.; Longo, A.; Liveri, V. T. *J. Phys. Chem. B* **2003**, *107* (1), 25.
(51) Nakaoka, Y.; Nosaka, Y. *Langmuir* **1997**, *13* (4), 708.
(52) Ma, Y.; Qi, L.; Ma, J.; Cheng, H. *Langmuir* **2003**, *19* (9), 4040.
(53) Bhattacharyya, S.; Kymakis, E.; Amaratunga, G. A. J. *Chem. Mater.* **2004**, *16* (23), 4819.

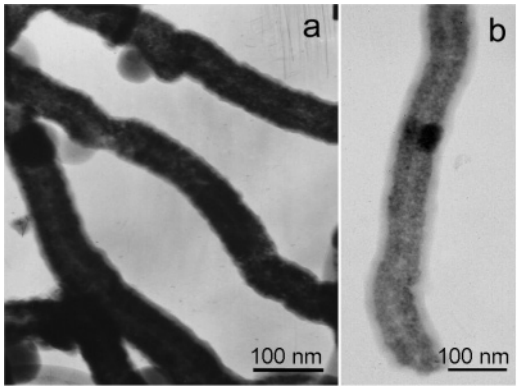

Figure 4. TEM images of the formed MWCNT/ZnS/SiO_2 heterostructures.

As a result of the unstable properties of sulfides in nature, it is critical to employ a protective sheath of thermally and chemically stable materials around the as-obtained products to enhance their performance for promising applications.[48,54,55] These MWCNT/ZnS heterostructures would benefit from having a silica shell to impart wettability and biocompatibility.[56−59] A silica shell should also minimize fluorescence quenching by surface adsorbates or redox-active molecules,[60−62] enabling them to be used in biosystems. Since Stöber et al. developed a method in which SiO_2 particles can form by the hydrolysis and polycondensation of tetraethoxysilane under alkaline conditions in ethanol,[63] various approaches have been reported for the preparation of coated inorganic nanoparticels (such as Au, ZnS, PbS, CdS, and CdTe).[48,54,59,64−66] The chemical process can be presented as

$$\mathrm{MWCNT/ZnS} + \mathrm{Si(OC_2H_5)_4} + \mathrm{NH_3} + \mathrm{2H_2O} \rightarrow \mathrm{MWCNT/ZnS/SiO_2} + \mathrm{4C_2H_5OH} + \mathrm{NH_3}$$

With the existence of water and ammonia, ethyloxysilane groups would hydrolyze into silanol groups(Si−OH), which would adhere to the surface of ZnS nanoparticles because of electrostatic forces. After SiO_2 coating, the uniform SiO_2 shell around the MWCNT/ZnS can be clearly observed, and tailored SiO_2 shell thickness in the range of 5−50 nm could be derived under controlled experimental conditions (Figure S7). Figure 4 shows typical TEM images for the MWCNT/ZnS/SiO_2 heterostructures with silica thicknesses of 5 and

(54) Wang, S. F.; Gu, F.; Lu, M. K. *Langmuir* **2006**, *22* (1), 398.
(55) Zhu, Y. C.; Bando, Y.; Yin, L. W. *Adv. Mater.* **2004**, *16* (4), 331.
(56) Chen, C. C.; Liu, Y. C.; Wu, C. H.; Yeh, C. C.; Su, M. T.; Wu, Y. C. *Adv. Mater.* **2005**, *17* (4), 404.
(57) Yi, D. K.; Selvan, S. T.; Lee, S. S.; Papaefthymiou, G. C.; Kundaliya, D.; Ying, J. Y. *J. Am. Chem. Soc.* **2005**, *127* (14), 4990.
(58) Barbé, C.; Bartlett, J.; Kong, L.; Finnie, K.; Lin, H. Q.; Larkin, M.; Calleja, S.; Bush, A.; Calleja, G. *Adv. Mater.* **2004**, *16* (21), 1959.
(59) Zhang, Y.; Li, Y. D. *J. Phys. Chem. B* **2004**, *108* (46), 17805.
(60) Nann, T.; Mulvaney, P. *Angew. Chem., Int. Ed.* **2004**, *43* (40), 5393.
(61) Chan, Y.; Zimmer, J. P.; Stroh, M.; Steckel, J. S.; Jain, R. K.; Bawendi, M. G. *Ad. Mater.* **2004**, *16* (23−24), 2092.
(62) Mulvaney, P.; Liz-Marzan, L. M.; Giersig, M.; Ung, T. *J. Mater. Chem.* **2000**, *10* (6), 1259.
(63) Stöber, W.; Frink, A.; Bohn, E. *J. Colloid Surf. Sci.* **1966**, *26*, 62.
(64) Correa-Duarte, M. A.; Giersig, M.; Liz-Marzan, L. M. *Chem. Phys. Lett.* **1998**, *286* (5−6), 497.
(65) Rogach, A. L.; Dattatri, N.; Ostrander, J. W.; Giersig, M.; Kotov, N. A. *Chem. Mater.* **2000**, *12* (9), 2676.
(66) Mulvaney, P.; Liz-Marzan, L. M.; Giersig, M.; Ung, T. J. *Mater. Chem.* **2000**, *10* (6) 1259.

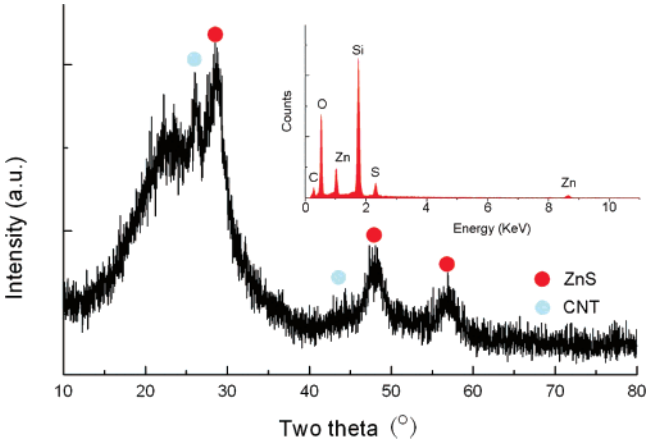

Figure 5. XRD pattern of the formed MWCNT/ZnS/SiO_2 heterostructures after heat-treated at 400 °C for 2h. Inset shows the corresponding EDS result of the sample.

10 nm, respectively. It is obvious that the MWCNT/ZnS composite nanowire is encapsulated by a uniform layer of silica. FTIR results confirmed the presence of SiO_2, CNT, and ZnS in the samples. Absorption bands at 466 (Si−O−Si band), 799 (Si−O−Si symmetric strength), 949 (Si−O−Si strength), and 1100 and 1195 cm^{-1} (Si−O−Si antisymmetric strengthes)[24] were observed after coating MWCNT/ZnS with SiO_2 (Figure S8). The data strongly suggested that the MWCNT/ZnS samples were really encapsulated within the silica matrix. To investigate the stability of the sample, we carried out the experiment by calcining the formed MWCNT/ZnS/SiO_2 heterostructures at 400 °C for 2 h. From the XRD pattern shown in Figure 5, almost all of the diffraction peaks are similar to those of the MWCNT/ZnS sample. The appearance of a strong, broad diffraction at lower angles ($2\theta = 21-26°$) can be attributed to the contribution of the amorphous silica sheath. No characteristic peaks of impurities such as zinc oxide were observed. EDS results also indicate the presence of Zn, S, C, O, and Si. These data clearly confirm that the obtained nanostructures still stayed stable even after heat treatment at 400 °C, which makes them appealing for practical applications in many fields. It should be noted that the luminescence intensity was enhanced greatly after coating MWCNT/ZnS with a SiO_2 layer while the peak position did not shift (Figure 3), which is terrific for biological applications. The enhancement of the luminescence intensity can be ascribed to the removal of electron capture centers on the surface of the ZnS sheath or the removal of nonradiative decay channels because of the silica shell around ZnS.

Conclusions

In summary, we have successfully prepared MWCNT/ZnS core/shell heterostructures by a facile solution−chemical method, which offers the possibility to readily control the thickness of the ZnS shell by adjusting the experimental parameters properly. The formation of ZnS shell on the MWCNTs has been found through the oriented aggregation of the formed ZnS nanocrystals. In addition, these heterostructures are easily encapsulated within a uniform SiO_2 layer without surface modification, showing better optical properties and thermal stability. Such special structures may enrich the family of 1D nanomaterials and represent good candidates for further applications.

Acknowledgment. This work was supported by the Shanghai Rising-Star Program (Grant 06QA14013), the National Natural Science Foundation of China (Grants 20236020 and 20176009), the Major Basic Research Project of Shanghai (Grant 04DZ14002), the Pre-973 Project of China (Grant 2002CCA2200), the 973 Project of China (Grant 2004CB719500), the Special Project for Key Laboratory of Shanghai (Grant 04DZ05622), and the Special Project for Nanotechnology of Shanghai.

Supporting Information Available: FTIR spectra of MWCNT/ZnS and MWCNT/ZnS/SiO_2 heterostructures; TEM images of MWCNTs, MWCNT/ZnS/SiO_2 heterostructures with different silica thicknesses, ZnS nanoparticles without MWCNTs, MWCNT/ZnS samples prepared without sonication; Raman spectra of MWCNT samples before and after sonication; and UV-vis absorption spectrum of MWCNT/ZnS heterostructures. This material is available free of charge via the Internet at http://pubs.acs.org.

IC7004858